

Carbon–lithium anodes for lithium secondary batteries

N. Imanishi*, S. Ohashi, T. Ichikawa, Y. Takeda and O. Yamamoto
Department of Chemistry, Faculty of Engineering, Mie University, Tsu 514 (Japan)

R. Kanno
Department of Chemistry, Faculty of Science, Kobe University, Kobe 657 (Japan)

(Received November 20, 1991; in revised form February 24, 1992)

Abstract

For the development of a superior anode for practical lithium secondary batteries, the carbon–lithium composite anode has been studied. As a carbon material, the carbon fiber M46 was mainly studied in this study. This material was proved to be highly reversible in comparison with other carbon materials. It is shown that lithium ions and/or solvated lithium ions intercalate into the fiber by using the X-ray diffraction (XRD) method and X-ray photospectroscopy (XPS) measurement. Coupled with the Cr_3O_8 cathode, a coin-type cell was constructed. Over 170 cycles were possible when the M46 carbon–lithium composite anode was used, whereas with the bare lithium metal anode only 80 cycles were observed. From the observation of scanning electron micrographs (SEM), it is shown that the carbon fiber prevents the formation of dendritic lithium metal.

Introduction

For the realization of lithium secondary batteries, there still exist some problems in the cathode material, electrolyte and anode material, respectively. Especially the anode cyclability has a great importance for the realization of the practical lithium secondary batteries. Except for the bare lithium anode, lithium–aluminium alloy or the suitable electrolyte for making the surface film on lithium metal have been used so far. These are used for covering the lithium metal surface in order to avoid the formation of lithium dendrites. This surface covering film must be highly reductive and stable. In this respect the carbon is most suitable for the anode material of lithium batteries [1]. As a carbon material, thermal decomposition products of polymers, such as polyphenylene and polyalylacetylene, will be good candidates because of their high surface area. By using these materials, better cell cyclability would be expected [2]. In this study, some carbon–lithium composite anodes were discussed, and the charge/discharge mechanisms were studied in detail.

Experimental

In this study, carbons thermally decomposed from polymers in our laboratory and commercial products were used. The former materials were produced from poly-

*Author to whom correspondence should be addressed.

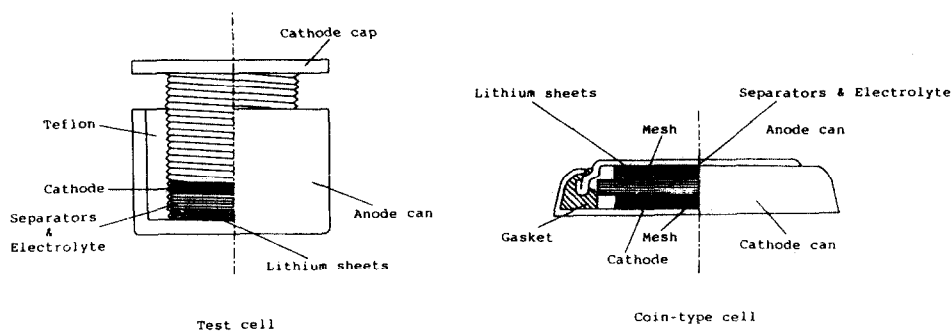


Fig. 1. The construction of the carbon test cell and coin-type cell.

phenylchloroacetylene (PPCA), polyvinylidene fluoride (PVDF), polyvinylidenechloride (PVDC), etc., by heating at 800 °C for 2 h under N_2 atmosphere. The latter materials were supplied from various companies and they are called M46, VM60019, A6000, etc. Before testing, these materials are ultrasonically pretreated in acetone and then dried. The preparation of the working electrode was as follows: the carbon material (50 mg) and polytetrafluoroethylene (PTFE) powder (5 mg) as a binding agent were mixed; this mixture was pressed under 100 kg cm^{-2} and formed into a disc shape (diameter 13.5 mm).

The cell construction is shown in Fig. 1. The two types of test cells were used. The cylindrical cell was used for the testing of the carbon fiber itself, while the commercial coin-type cell was used for testing the characteristics as a secondary lithium battery. In both cases, the counter electrode was a lithium foil and the electrolyte was 1:1 propylenecarbonate (PC)-dimethoxyethane (DME) containing 1 M $LiClO_4$. The separator was a microporous polypropylene sheet. The pellet of Cr_3O_8 was used as a cathode for the lithium secondary battery with the carbon–lithium composite anode. This cathode was prepared by the thermal decomposition of CrO_3 in an autoclave [3].

The materials obtained were characterized by using X-ray diffraction (XRD), BET adsorption measurement, scanning electron micrograph (SEM) and XPS. The electrochemical measurements were carried out using a potentiostat. In the galvanostatic mode, the cutoff voltage was -0.03 V in charge and 2.5 V in discharge versus Li/Li^+ . The current density was $350 \mu\text{A cm}^{-2}$. The open-circuit voltage (OCV) was measured after a discharge of specific capacity and 1 day duration. All the procedures were performed in an argon atmosphere dry box.

Results and discussion

At first, the charge/discharge characteristics of the carbon electrode was examined. In Fig. 2 are shown the discharge OCV and the charge/discharge curves of lithium and thermally-decomposed PPCA carbon cells. On charging the cell voltage decreased rapidly in an early period, but decreased slowly from c. 1 V to 0 V. This suggests that some electrochemical reaction occurs in this voltage region. When the carbon was discharged successively the voltage rapidly increased to 2.5 V. This results show that only a little part of the charged lithium could be discharged. The OCV curve indicates that in the early period, the overvoltage was very large. On the other hand,

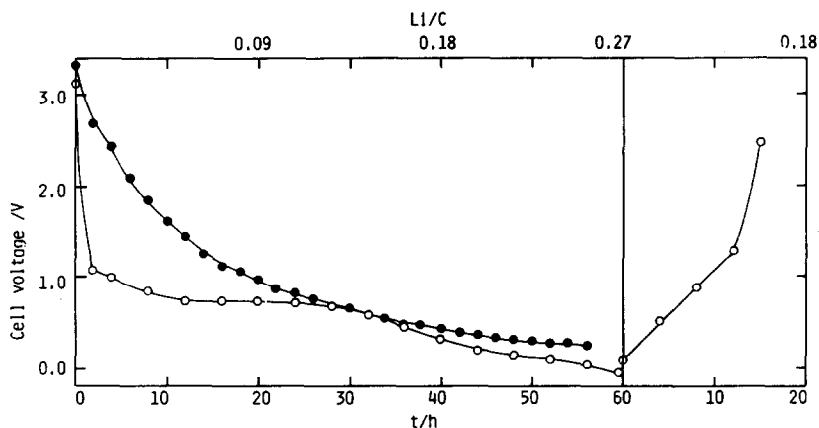


Fig. 2. The charge/discharge closed-circuit voltage (CCV) and open-circuit voltage (OCV) curves for the cell lithium/carbon (PPCA) with current density 0.35 mA cm^{-2} . (○) CCV; (●) OCV.

it became very small after 20 h charge. As mentioned before, the charge mechanisms of the carbon seemed to be different between the higher and lower voltage regions. What sort of reaction would occur in the course of charge is not clear at present.

The large capacity in the first charge may be partly due to adsorption onto the surface of the carbon and partly due to intercalation into the van der Waals gap of the graphite-like structure. Thus, it is important to know the surface area of the carbon examined. The surface area of the carbons, measured by the BET method, are listed in Table 1. In the case of the thermal decomposition carbons, except for PPCA, the storage capacities at the first cycle increased with increasing surface area. From these results, the lithium charge capacity of the thermal decomposition products depends mainly on the lithium adsorption capacity on the carbon surface. The lithium storage is probably explained by charging the double layers on the carbon electrodes. Loss of capacity on following cycles indicates that lithium adsorption onto the surface is an irreversible reaction. The reversible cyclability is not accomplished by a surface reaction and we suppose that the intercalation reaction brings high reversibility. In the case of PPCA, no significant decrease of capacity could be observed after second cycle. This shows that the electrode reaction mechanism is different from those of the other thermal decomposition carbons. On the other hand, the surface areas of the commercial carbon fibers are extremely small in comparison with those of the thermal decomposition carbons. Moreover, loss of capacity was much smaller than thermal decomposition carbons. These results show that the lithium intercalation was a predominant reaction in the commercial fibers. The highest efficiency was observed for the carbon fiber M46. In the case of PPCA and M46, the reaction of lithium intercalation into the host matrix is considered to contribute to the high charge capacity. The cycle test for PPCA showed good rechargeability only over 50 cycles, while the M46 showed over 1000 cycles. We conclude that M46 is a candidate for the anode of lithium secondary batteries.

The charge mechanisms of the carbon fiber M46 were studied by the XRD method. Figure 3(a) shows the XRD patterns at various charge capacities. The (002) peak

TABLE 1

Lithium storage capacities of thermal decomposition products of polymers and carbon fibers

Polymer or carbon fiber	Charge capacity (m Ah 100 mg ⁻¹) cycle number			Discharge capacity (m Ah 100 mg ⁻¹) cycle number			Surface area (m ² g ⁻¹)
	1	3	5	1	3	5	
Thermal decomposition polymers							
PPCA	59.6	13.5	14.6	15.7	12.4	13.6	430
PVDF	67.8	8.3	4.3	8.2	6.5	3.8	880
PVDC	57.7	5.1	2.4	5.5	3.4	2.2	510
POB	58.0	2.1	1.4	5.8	2.1	1.6	280
PS	36.8	2.6	1.6	5.0	2.9	1.5	100
PEPY	10.8	1.2	0.8	1.0	0.9	0.6	6
PVC	27.0	0.8	0.6	5.0	0.7	0.6	4
Graphite	14.0	1.0	0.5	0.8	0.6	0.4	4
Carbon fiber							
M46	18.5	7.3	8.4	8.3	7.1	8.1	1.3
T300 ^{a)}	21.8	3.5	1.1	2.3	0.8	0.5	1.6
GM60019	22.4	5.8	3.5	6.2	5.1	3.1	1.3
HTA-7	43.9	6.8	4.7	15.9	5.6	4.0	3.6
GM6060ST ^{b)}	13.8	3.4	3.1	6.6	3.0	2.8	0.7
GF8 ^{c)}	24.2	1.4	1.2	4.9	1.1	0.8	0.4
A6000 ^{d)}	33.8	0.5	0.3	7.4	0.3	0.4	4.9
HTA-7	28.4	3.2	3.1	10.5	3.2	2.8	3.6
BP1034AES ^{e)}	13.6	0.5	0.2	11.0	0.4	0.1	1.1

^aToray Industries, Inc.^bToa Nenryo Kogyo, kk.^cNippon Carbon Co., Ltd.^dAsahi Nippon Carbon Co., Ltd.^eToho Rayon Co., Ltd.

PPCA: poly[2-chloro-1-phenylacetylene]; PVDF: polyvinylidene fluoride; PVDC: polyvinylidene chloride; POB: polyoxybenzoate; PS: polysulfon; PEPY: polyetherpolyimide; PVC: polyvinyl chloride.

shifted to lower angles with deeper charge, indicating the inter-layer expansion along the *c*-axis. The intercalation of lithium ions and/or solvated lithium ions into the van der Waals gap would occur. The *d*-values of the (002) peak are plotted against the charge capacity in Fig. 3(b). This shows that the lithium charge reaction with M46 proceeds via three steps. First, for $x(\text{Li}/\text{C}) < 0.05$, lattice expansion was not observed. In this early region the lithium intercalation reaction did not proceed. This indicates that the surface reaction such as lithium adsorption occurred. For $0.05 < x < 0.14$, a linear increase of *d*-value was observed. In the carbon fiber M46, the structure does not have a graphite-type regular arrangement [4, 5]. The staging structure does not appear and the peak seemed to be the average of all the (002) peaks which have different level of expansion. In this charging stage, the lithium intercalation might occur and highly reversible characteristics could be expected. For $x > 0.14$, no further lattice expansion could be observed. In this region, the lithium ions have already fully

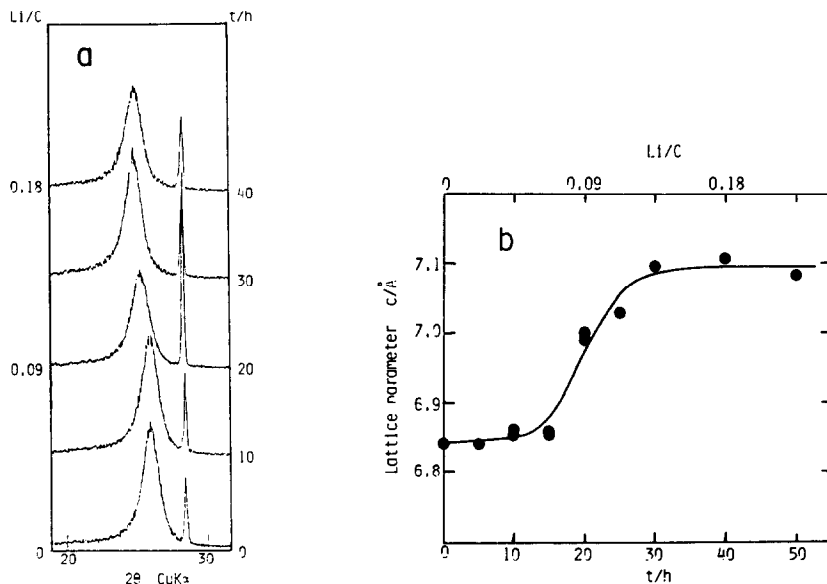


Fig. 3. (a) X-ray diffraction patterns of the carbon fiber M46 at different lithium capacities; (b) the change of the d -value of the carbon fiber M46 through the charge.

intercalated into the van der Waals gap and, consequently, lithium metal deposits onto the surface of the carbon fibers.

For the thermal decomposition product of PPCA, lithium intercalation into the electrode could not be confirmed by the XRD data. But the change in the binding energy observed for XPS measurements suggests the same reaction mechanism as in the M46 material.

In Fig. 4, the XPS spectra of the Li 1s and C 1s were measured for M46 at various capacities. At the early stage of the charge, the binding energy of the Li ($E_b = 54.89$ eV) is close to that of metallic lithium ($E_b = 54.69$ eV). This shows that at the first stage of charge ($x < 0.05$), the lithium exists in a metallic state and/or some reaction products with small binding energy. The peak shifts to higher energy with lithiation ($x > 0.05$) and the maximum value ($E_b = 55.49$ eV) is obtained around $x = 0.09$. This lithium is deduced to be the intercalated one and is in different state from the lithium at the early stage. Also at this capacity, the cyclability showed the highest efficiency. For $x > 0.14$ the binding energy of lithium was reduced again and its value became as same as that of metallic lithium. Lithium metal deposition would happen in this region. This lithium did not show the good reversibility.

For the C 1s spectra, a new peak with a higher binding energy ($E_b = 285.7$ eV) was observed for the lithiated carbon besides the original carbon peak. The height of the new peak increased with charging and became a maximum at around $x = 0.09$. The M46 showed the highest efficiency in rechargeability at this point as mentioned above.

The XPS data on the PPCA material suggest that the charge also proceeds by the same electrode reaction. The lithium peak shifts to higher energy with lithiation and the highest binding energy was observed at $x = 0.21$, where the cell showed the highest efficiency in rechargeability. In a deeper charge, the peak shifts again to lower

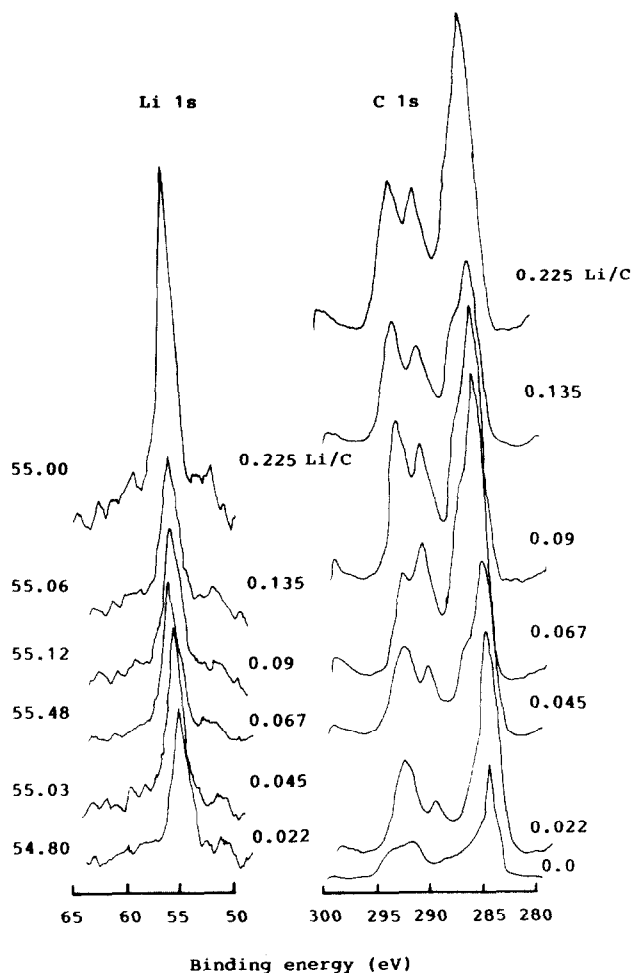


Fig. 4. The XPS spectra of the carbon fiber M46 at different lithium capacities.

energy. At this point lithium metal deposits on the surface of the PPCA. The reactions of the PPCA are intrinsically the same as that of the M46 and the difference for the charge/discharge characteristics between these materials arises from the degree of the random orientation in the carbon crystal. The M46 is more suitable for lithium intercalation than other carbon materials.

From all of these results, the M46 is a suitable material for the anode active material of the lithium secondary batteries. In order to estimate the cyclability when loaded in a practical coin-type cell, cell testing was carried out. Cr_3O_8 was used as cathode material, and M46 and lithium composite electrode as an anode. In Fig. 5, the charge/discharge curves of the $\text{Li}/\text{Cr}_3\text{O}_8$ cell and $\text{Li-carbon}/\text{Cr}_3\text{O}_8$ cell are compared. For the cells using lithium metal, 80 cycles were obtained, while for the composite anodes, more than 170 cycles were obtained, twice those for the cell with only lithium anode. The carbon-lithium composite anode improves the cycling efficiency in lithium secondary batteries. After the cycling test, the surface of the anode was

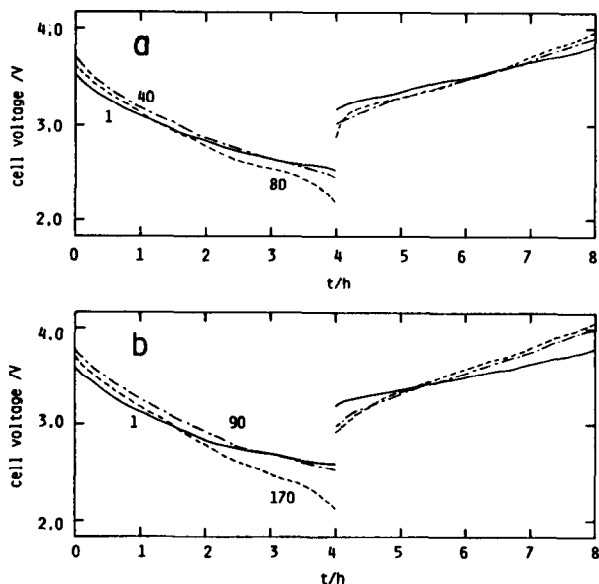


Fig. 5. The charge/discharge cycles of the cell using Cr_3O_8 as a cathode: (a) $\text{Li}/\text{Cr}_3\text{O}_8$; (b) $\text{Li-M46}/\text{Cr}_3\text{O}_8$.

covered with dendritic lithium when only lithium metal used. On the other hand, for the carbon-lithium anode, no formation of dendrites was observed. The use of M46 carbon fiber hindered significantly the formation of lithium dendrites.

In conclusion, the carbon anodes can accommodate lithium ions and/or solvated lithium ions into their matrix. For M46 the lithium intercalation occurred at the utilization range $0.05 < x < 0.14$ and the cycle efficiency showed the highest value in this region. Applying these characteristics to the reversible anode of lithium secondary batteries, the lithium dendrite formation was reduced and the cycle efficiency of the $\text{Li-carbon}/\text{Cr}_3\text{O}_8$ cell was improved. In fact, it has been proved that the $\text{Li-carbon}/\text{Cr}_3\text{O}_8$ cell showed improved cycle efficiency. However, it is not clear what structure is most suitable for the lithium reversibility, and it is necessary to know in detail the structure of the carbon and the lithium as an intercalant to develop better carbon materials.

Acknowledgements

We gratefully acknowledge the support of the Nissan Science Foundation.

References

- 1 J. O. Besenhard and H. P. Frits, *Angew. Chem., Int. Ed. Engl.*, 22 (1983) 950.
- 2 F. P. Dousek, J. Jansta and J. Baldrian, *Carbon*, 18 (1980) 13.
- 3 K. A. Wilhelm, *Acta Chem. Scand.*, 22 (1968) 2565.
- 4 Y. Matsuda, M. Morita and H. Katsuma, *Denki Kagaku*, 51 (1983) 744.
- 5 F. Beck, H. Junge and H. Krohn, *Electrochim. Acta*, 26 (1981) 799.